nature chemical biology

ARTICLE

PUBLISHED ONLINE: 17 JANUARY 2010 | DOI: 10.1038/NCHEMBIO.307

Rapid behavior-based identification of neuroactive small molecules in the zebrafish

David Kokel[1,2]*, Jennifer Bryan[3,4], Christian Laggner[5], Rick White[3], Chung Yan J Cheung[1,2], Rita Mateus[1,2], David Healey[1,2], Sonia Kim[1,2], Andreas A Werdich[1], Stephen J Haggarty[2,6,7], Calum A MacRae[1], Brian Shoichet[5] & Randall T Peterson[1,2]*

Neuroactive small molecules are indispensable tools for treating mental illnesses and dissecting nervous system function. However, it has been difficult to discover novel neuroactive drugs. Here, we describe a high-throughput, behavior-based approach to neuroactive small molecule discovery in the zebrafish. We used automated screening assays to evaluate thousands of chemical compounds and found that diverse classes of neuroactive molecules caused distinct patterns of behavior. These 'behavioral barcodes' can be used to rapidly identify new psychotropic chemicals and to predict their molecular targets. For example, we identified new acetylcholinesterase and monoamine oxidase inhibitors using phenotypic comparisons and computational techniques. By combining high-throughput screening technologies with behavioral phenotyping *in vivo*, behavior-based chemical screens can accelerate the pace of neuroactive drug discovery and provide small-molecule tools for understanding vertebrate behavior.

Neuroactive drugs discovered in the 1950s revolutionized our understanding of the nervous system and the treatment of its disorders[1]. Most of these drugs were discovered serendipitously when they produced unexpected behavioral changes in animals or humans. Elucidation of the targets of these behavior-modifying compounds led to insights into nervous system function, and many of the drugs used for treating nervous system disorders today were derived from those same, serendipitous discoveries.

Unfortunately, few new classes of neuroactive molecules have been discovered in the last 50 years, in part because pharmaceutical discovery efforts are dominated by simple, *in vitro* screening assays that fail to capture the complexity of the vertebrate nervous system[2]. Current drug discovery approaches are typically target based, meaning they seek to identify compounds that modify the *in vitro* activity of a specific protein target. These approaches benefit from being systematic and high throughput. However, they generally lack the ability to discover drugs that modify nervous system function in new ways.

Unlike target-based approaches, phenotype-based screens can identify compounds that produce a desired phenotype without a priori assumptions about their targets. Phenotype-based screens in cultured cells and whole organisms have identified powerful new compounds with novel activities on unexpected targets *in vivo*[3]. However, it has been difficult to combine chemical-screening paradigms with behavioral phenotyping, perhaps because many well studied behaviors are too variable or occur in animals that are too large for screening in multi-well format.

A common limitation of compounds discovered by phenotype-based methods is the difficulty in determining their mechanisms of action. It has been proposed that systems-level analyses of content-rich phenotypic data could be used to identify mechanistic similarities between compounds and predict their mechanisms of action[4]. Repositories of high-throughput screening data such as PubChem and ChemBank are beginning to make such analyses possible, but difficulties remain, including the challenges of comparing phenotypes across disparate assay types, libraries and experimental conditions. Theoretically, the behavioral effects of small molecules could provide sufficient content to enable compound characterization and prediction of their mechanisms of action. However, because behaviors can be complex and difficult to quantify, systems-level comparison of behavioral phenotypes would require conversion of the behaviors into simple, quantitative measures that are more amenable to such approaches.

Given the unmet need for novel psychotropic drugs, we sought to develop a small-molecule discovery process that combined the scale of modern high-throughput screening with the biological complexity of behavioral phenotyping in living animals. Here, we report development of a fully automated platform for analyzing the behavioral effects of small molecules on embryonic zebrafish. Using this platform, we have identified hundreds of behavior-modifying compounds. We further demonstrate that complex behavioral changes can be distilled into simple behavioral 'barcodes' to classify psychotropic drugs and determine their mechanisms of action.

RESULTS

The photomotor response

We discovered that a high-intensity light stimulus elicits a stereotypic series of motor behaviors in embryonic zebrafish that we call the photomotor response (PMR) (**Fig. 1a**,**b** and **Supplementary Movies 1–3**). The PMR can be divided into four broad phases: a pre-stimulus background phase, a latency phase, an excitation phase and a refractory phase (**Fig. 1c**). During the pre-stimulus phase, zebrafish embryos were mostly inactive, showing low basal activity characterized by spontaneous and infrequent body flexions within their chorions. Presentation of a light stimulus elicited a robust motor excitation phase (lasting 5–7 s) characterized by vigorous

[1]Cardiovascular Research Center and Division of Cardiology, Department of Medicine, Massachusetts General Hospital, Harvard Medical School, Charlestown, Massachusetts, USA. [2]Broad Institute, Cambridge, Massachusetts, USA. [3]Department of Statistics and [4]Michael Smith Laboratories, University of British Columbia, Vancouver, British Columbia, Canada. [5]Department of Pharmaceutical Chemistry, University of California, San Francisco, California, USA. [6]Center for Human Genetic Research, Massachusetts General Hospital, Boston, Massachusetts, USA. [7]Stanley Center for Psychiatric Research, Cambridge, Massachusetts, USA. *e-mail: dkokel@cvrc.mgh.harvard.edu or peterson@cvrc.mgh.harvard.edu

shaking. This excitation phase was preceded by a latency phase (lasting 1–2 s) and was followed by a refractory phase during which basal activity was suppressed and embryos did not respond to a second light pulse (**Fig. 1a**). We found that the PMR consistently occurred in almost all untreated embryos and that the PMR assay could be scaled to 96-well plate format (**Fig. 1d**).

To quantify the effects of small molecules on the PMR, we selected 14 quantitative features that can be automatically extracted from the behavioral recordings (**Fig. 1c**). The 14 features are derived from the motion of embryos during seven periods of time, including one period during the pre-stimulus background phase, one period during the latency phase, three periods during the excitation phase and two periods during the refractory phase (**Fig. 1c**). For each of the seven time periods, we identified the first and third quartiles of the motion index. These features were compared to the control population and depicted as a sequence of 14 pseudo-*z* scores (which we call a 'barcode') representing the effect of a compound on motor activity (**Fig. 1c**). Barcodes facilitated the analysis of large-scale data sets by providing a concise quantitative summary of the behaviors observed in each well (**Fig. 1e**).

Effects of small molecules on the PMR

We found that known psychoactive drugs altered the PMR in distinct and reproducible ways (**Fig. 2**). For example, isoproterenol (**1**), a psychostimulant, increased motor activity throughout the PMR, whereas diazepam (**2**), an anxiolytic, decreased activity (**Fig. 2a–i**). The dopamine agonist apomorphine (**3**) lengthened the PMR latency period, whereas the cardenolide digitoxigenin (**4**) caused a vigorous and prolonged motor response to the stimulus (**Fig. 2j–o**). Embryos exposed to 6-nitroquipazine (**5**), a serotonin reuptake inhibitor, showed a robust but brief motor response to the first stimulus but, unlike untreated embryos, also responded to the second stimulus (**Fig. 2p–r**). All of these small molecule–induced behavioral effects were statistically significant and reproducible across different days and different embryos (**Fig. 2**, right column, and **Supplementary Table 1**). We found that many neuroactive compounds showed activity between 10 μM and 100 μM in this assay, whereas they lost activity at lower concentrations (**Supplementary Fig. 1**) and sometimes induced toxicities at higher concentrations (**Supplementary Fig. 1**, digitoxigenin). These data show that small molecules with different mechanisms of action (for example, adrenergic, dopaminergic and serotonergic) produce distinct changes in the PMR assay, suggesting the involvement of multiple neurotransmitter pathways in the various components of the PMR. Thus, despite the novelty of this behavior, we reasoned that the PMR might have predictive value for neuroactive drug discovery.

High-throughput, behavior-based chemical screening

To determine whether high-throughput behavioral phenotyping could be used to identify novel neuroactive drugs and their mechanisms of

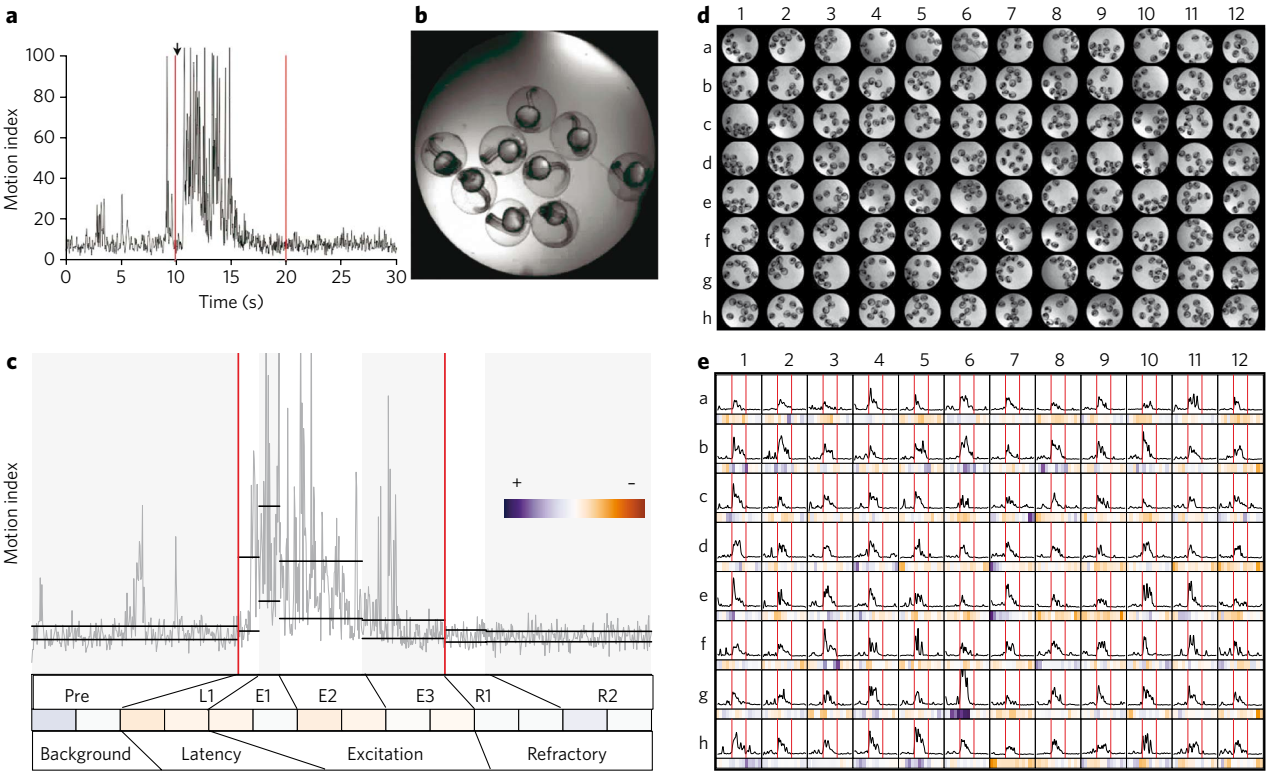

Figure 1 | The PMR and high-throughput behavioral barcoding. (**a**) Representative plot of the aggregate motor activity (in arbitrary units) over time from all embryos in a single control well during the PMR assay. Before the first light stimulus (red line at 10 s), brief asynchronous movements in individual embryos appear as narrow spikes with short (<1 s) duration. A latency phase, lasting for approximately 1 s (arrow), exists between the first light pulse and the onset of the excitation phase. The PMR excitation phase is clearly distinguished from background as a large, sustained increase in motor activity. After the excitation phase, embryos enter a refractory phase in which a second light pulse (red line at 20 s) does not elicit a response. (**b**) Nine zebrafish embryos in a single well of a 96-well plate. (**c**) PMR plot from a representative untreated control well. The motion index profile for each well was partitioned into seven periods: PRE, L1, E1, E2, E3, R1, R2. For each period, the motion index values for each well were summarized in two features, Q1 (lower line, first bar in barcode) and Q3 (upper line, second bar in barcode), which are the first and third quartiles, respectively. This 14-number summary formed the behavioral barcode. Colors in the heat map represent deviation from the average control phenotype: purple, higher activity; orange, lower activity. (**d**) Composite photograph of a 96-well microtiter plate before behavioral analysis. Each well contains 8–10 unhatched zebrafish embryos. (**e**) PMR profiles and the respective behavioral barcodes of 96 untreated control wells.

action, we used the PMR and an additional embryonic touch response (ETR) assay (see Methods) to assess the behavioral phenotypes of zebrafish embryos exposed to 14,000 different small molecules. To evaluate the behavioral effects of such a large number of compounds, we built a high-throughput, automated platform capable of screening approximately 5,000 embryos per microscope-day (**Supplementary Table 2** and **Movie 4**). Together, we collected behavioral information from over 25,000 wells, representing the behaviors of more than a

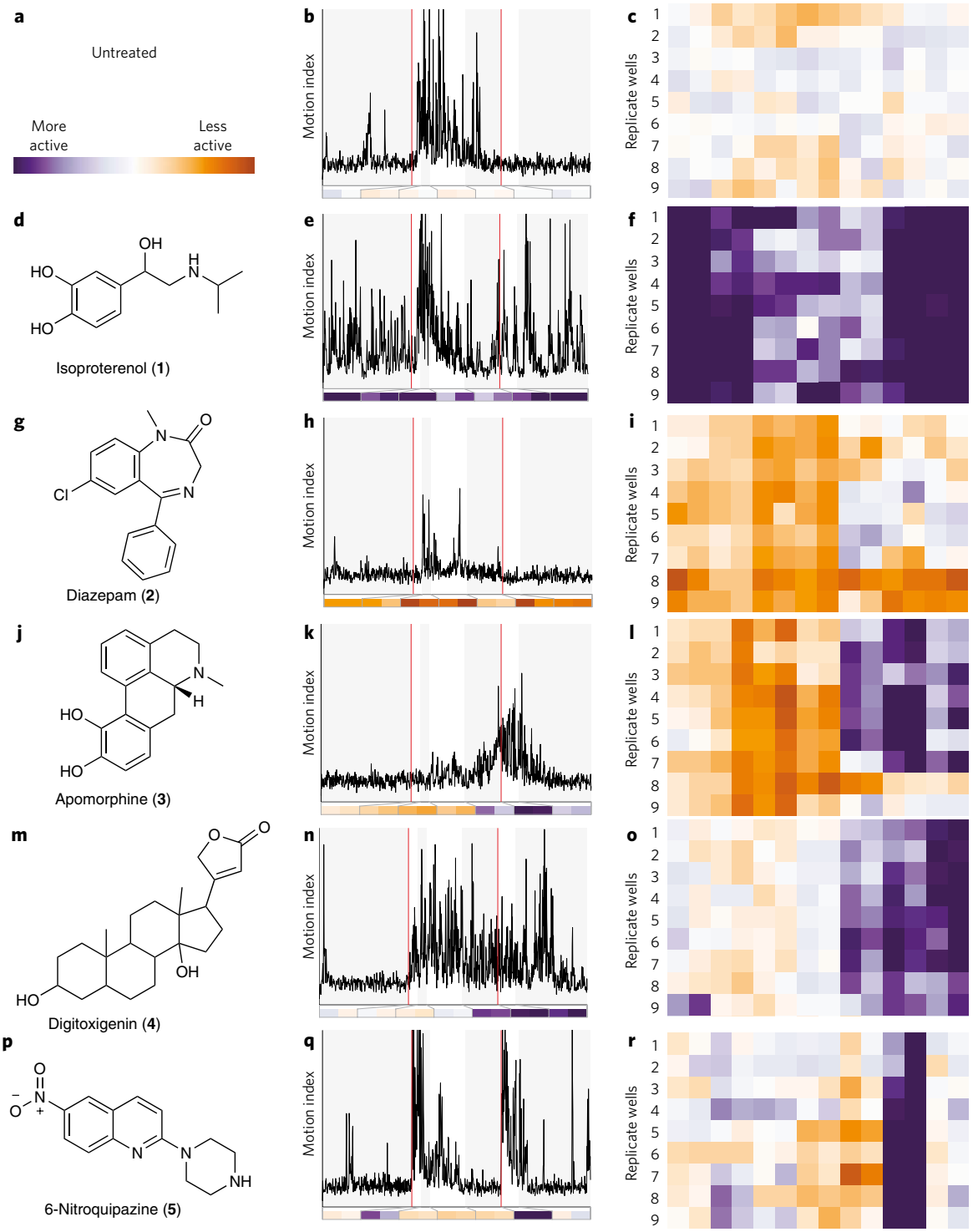

Figure 2 | Neuroactive chemicals cause specific patterns of behavior. (**a**) Heat map color key. Colors in the heat map represent deviation from the average control phenotype: purple, higher activity; orange, lower activity. (**b**) PMR plot from a representative untreated control well and its associated barcode. (**c**) Behavioral barcodes from nine independent untreated control wells. (**d**–**f**) Isoproterenol, a psychostimulant, increased zebrafish motor activity ($P = 6.53 \times 10^{-8}$). (**g**–**i**) Diazepam, an anxiolytic, reduced motor activity ($P = 2.33 \times 10^{-7}$). (**j**–**l**) Apomorphine, a dopamine agonist, increased PMR latency period duration ($P = 1.88 \times 10^{-6}$). (**m**–**o**) Digitoxigenin, a cardiotonic steroid, prolonged duration of the PMR excitation phase ($P = 6.03 \times 10^{-7}$). (**p**–**r**) 6-Nitroquipazine, an SSRI, modulated the PMR refractory period ($P = 6.73 \times 10^{-7}$). (**b**,**e**,**h**,**k**,**n**,**q**) Representative PMR plots and their corresponding barcodes from wells treated with the indicated compounds. (**c**,**f**,**i**,**l**,**o**,**r**) Nine replicate behavioral barcodes from independent wells treated with the indicated compound.

quarter million embryos. The similarity of barcodes obtained from independent wells treated with the same chemical was substantially and significantly higher than background well-to-well similarity ($P < 1 \times 10^{-70}$; **Supplementary Fig. 2**), suggesting good assay reproducibility. We identified 1,627 wells (a 7% hit rate) in which at least one behavioral feature was statistically distinct from control wells (which had a 2.5% false-positive rate). Overall, 56% of hits (655 unique molecules) caused various patterns of increased activity, whereas the remaining 44% of hits (327 unique molecules) were generally sedating (**Fig. 3a**). Although many of the molecules that reduced activity in the PMR assay were also annotated as causing a toxic phenotype, other molecules, including known anesthetics and analgesics, were annotated as healthy sedatives in the ETR screen (**Fig. 3a**) per observation of sedation without severe cardiovascular depression or other obvious toxicities.

Systems-level analysis of behavior-modifying molecules

Hierarchical clustering was used to organize compounds into clusters of phenotypically related molecules. For all featured clusters, we formally compared the featured barcodes with those observed in control wells and confirmed that these groups represented statistically distinct and coherent sets of behavior-modifying molecules (**Supplementary Table 1**). We found that clusters of barcodes representing similar phenotypes (phenoclusters) were often enriched with functionally related compounds (**Fig. 3b–e**). For example, one phenocluster, characterized by elevated activity in all PMR phases, was largely composed of beta-adrenergic receptor (ADBR) agonists, including isoproterenol, clenbuterol (**6**) and epinephrine (**7**) (**Fig. 3c**). As expected, beta-blockers had the opposite effect and generally decreased motor activity (**Supplementary Fig. 3**). A second phenocluster, characterized by a prolonged latency period, was highly enriched for dopamine

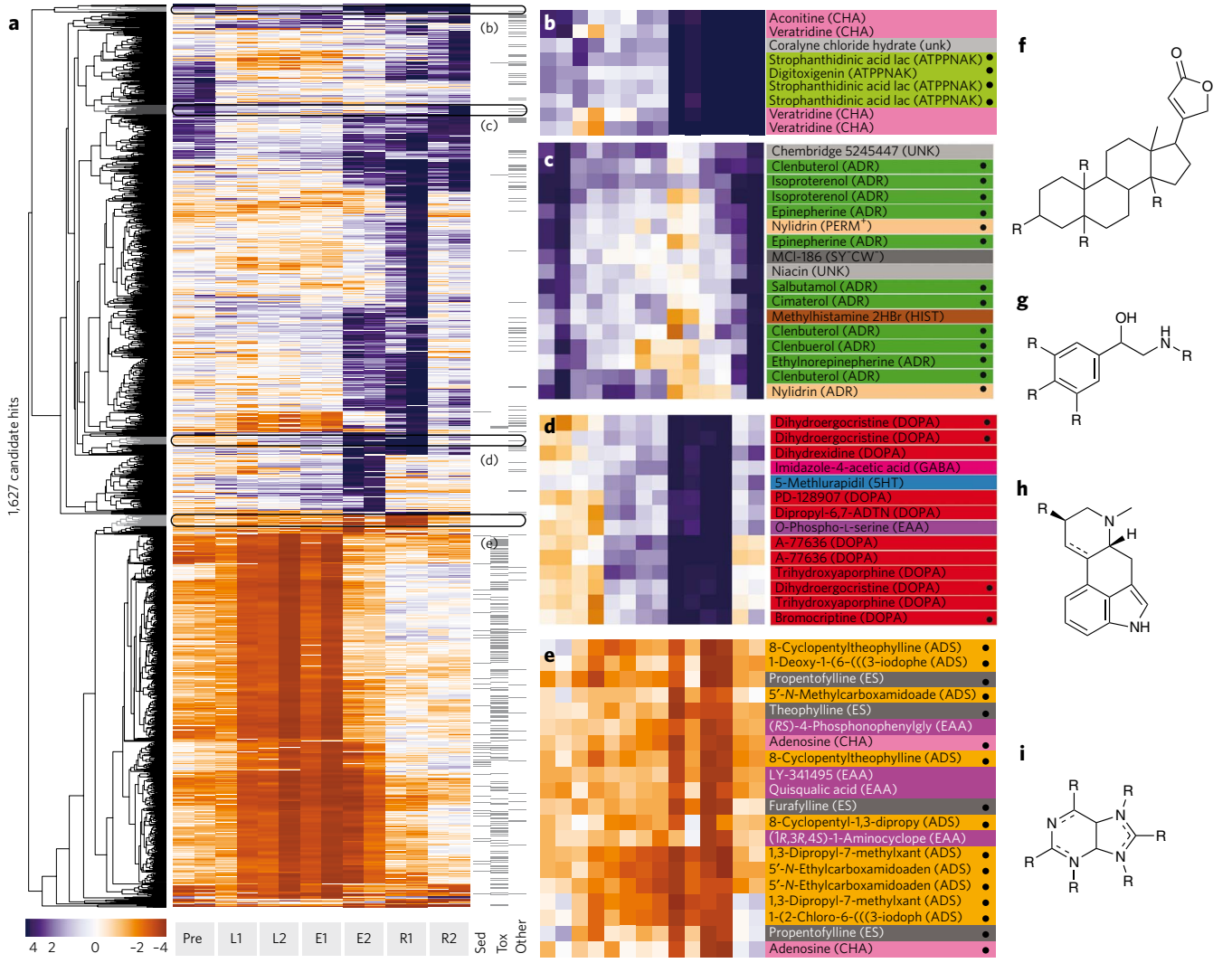

Figure 3 | Hierarchical clustering reveals that compounds cluster with functionally similar molecules. (**a**) A dendrogram of behavioral barcodes for all 1,627 hits clustered by phenotypic similarity. Candidate hits (*y* axis) are clustered on the basis of behavioral features (*x* axis) from the PMR assay. Gray bars denote the presence of the indicated phenotypes in the ETR assay: Sed, sedation; Tox, toxicity. The four clusters circled on the dendrogram are shown at higher resolution in panels **b**–**e**. Chemical names are colored according to the activity code annotations in parentheses. Compounds without functional annotation are labeled unknown (unk). (**b**) A phenocluster showing excitation period prolongation is enriched for compounds that alter intracellular sodium concentrations ($P = 4.71 \times 10^{-7}$). Inhibitors of Na^+ channel inactivation (CHA) and the Na^+/K^+ pump (ATPPNAK) are colored pink and light green, respectively. (**c**) A cluster showing generalized stimulation is enriched ($P = 9.94 \times 10^{-14}$) for β-adrenergic receptor agonists (ADR, dark green). (**d**) A cluster showing prolonged latency is enriched ($P < 2.2 \times 10^{-16}$) for dopamine receptor agonists (DOPA, red). (**e**) A cluster showing attenuated excitation is enriched ($P < 2.2 \times 10^{-16}$) for adenosine receptor antagonists (ADS, orange). Indicated compounds (●) are structural analogs of the scaffold shown to the right of each cluster in **f**–**i**. $PERM^+$, membrane permeability inhibitor; HIST, histaminergic; GABA, GABAergic; 5HT, serotonergic; EAA, glutamatergic; ES, esterase inhibitor; SY^-CW^-, cell wall synthesis inhibitor.

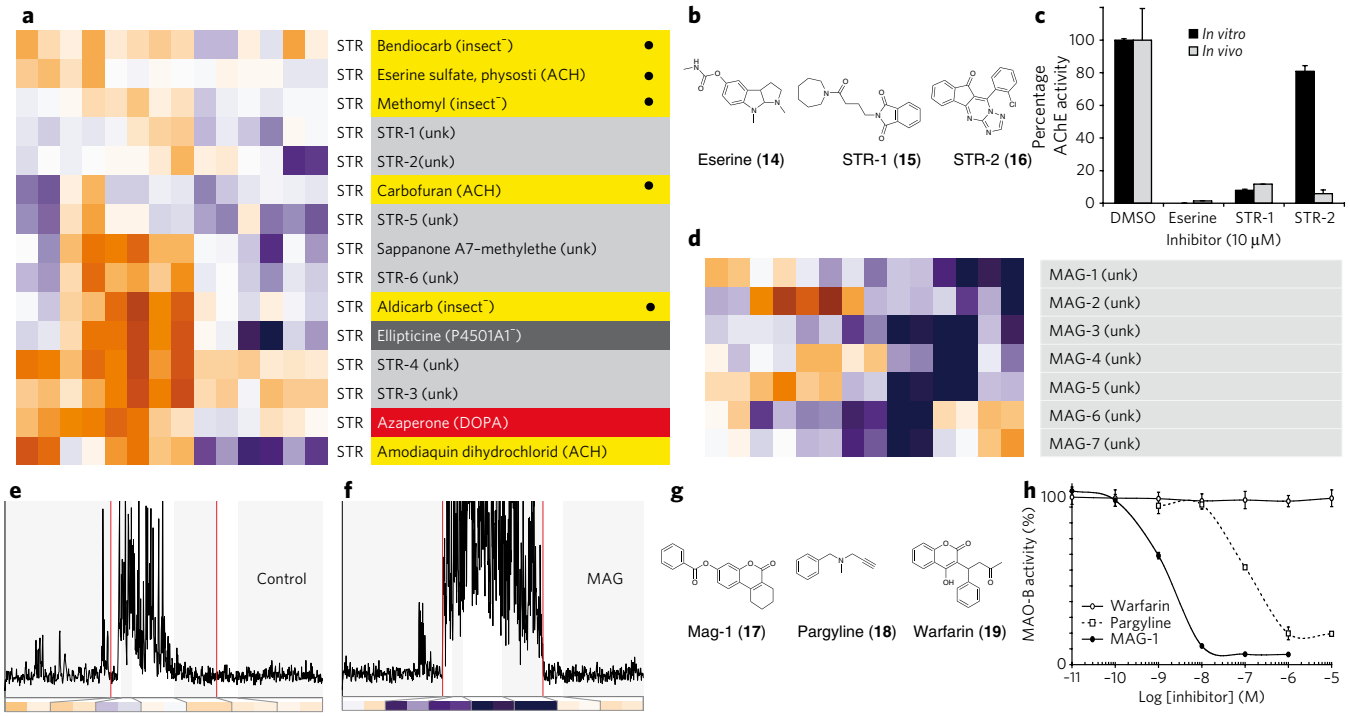

Figure 4 | Behavior-based discovery of novel neuroactive small molecules. (**a**) Behavioral barcodes of chemicals causing the STR phenotype (P = 0.00034). Known AChE inhibitors are colored yellow. Insect⁻, insecticide; ACH, AChE inhibitor; P4501A1, cytochrome P450 activated. (**b**) Structures of eserine, a known AChE inhibitor, and two previously uncharacterized compounds that also cause the STR phenotype, STR-1 and STR-2. (**c**) AChE activity *in vitro* or *in vivo*. Data represent mean values ± s.d. (**d**) Behavioral barcodes of structurally related MAG compounds. (**e**,**f**) Representative PMR plots of a control well (**e**) and a MAG compound–treated well (**f**). There is a stimulus-dependent increase in excitation magnitude and duration. (**g**) Chemical structures of the known MAO inhibitor pargyline, of MAG-1 and of warfarin, a negative control. (**h**) MAO-B activity after treatment with the indicated compounds. Data points and error bars represent mean values ± s.d. Curves were fit using Bezier spline smoothing.

agonists, including dihydroergocristine (**8**), dihydrexidine (**9**) and compound PD128907 (**10**) (**Fig. 3d**). A third cluster, characterized by an abbreviated PMR excitation period, was enriched for adenosine receptor antagonists (**Fig. 3e**). In addition to sharing common mechanisms of action, many of these compounds also share common chemical scaffolds (**Fig. 3f–i**). Thus, behavioral barcodes can be used to sort molecules into biologically relevant functional classes.

Because functionally related molecules cause similar phenotypes, behavioral barcodes may be used to sort molecules with different cellular targets into common pathways. For example, we identified a phenocluster characterized by prolongation of the PMR excitation period that included aconitine (**11**), veratridine (**12**), strophanthidinic acid (**13**) and digitoxigenin (**Fig. 3b**). Aconitine and veratridine are inhibitors of voltage-gated sodium channel inactivation, whereas strophanthidinic acid and digitoxigenin are inhibitors of the Na^+/K^+ ATPase[5,6]. How these molecules with different cellular targets generate the same behavioral phenotype is unknown. However, both types of molecule are predicted to increase intracellular Na^+ concentration. It is possible that these related mechanisms could underlie their phenotypic similarity.

Target identification for novel hits

We hypothesized that behavioral barcodes could be used to predict mechanisms of action for novel behavior-modifying compounds. To test this possibility, we looked for clusters containing both well characterized and completely uncharacterized molecules. For example, we identified fifteen molecules that all caused a distinctive slow-to-relax (STR) phenotype in the ETR assay (**Fig. 4a**). The STR phenotype involves prolonged tail flexion and a slow return to the relaxed state (**Supplementary Movies 5** and **6**). Several of these compounds, including eserine (**14**), are known to inhibit acetylcholinesterase (AChE), whereas two other compounds, STR-1 (**15**) and STR-2 (**16**), are structurally unrelated molecules with no known activity in animals (**Fig. 4a**,**b**). The clustering of STR-1 and STR-2 with known AChE inhibitors suggested that these novel compounds might inhibit AChE. To test this possibility, we determined the activity of these molecules in AChE activity assays. STR-1 inhibited AChE activity *in vitro* (half-maximal inhibitory concentration (IC_{50}) = 500 nM), confirming that it is a novel AChE inhibitor (**Fig. 4c** and **Supplementary Fig. 4a**). Interestingly, a high concentration of STR-2 (10 μM) did not inhibit purified AChE *in vitro* (**Fig. 4c** and **Supplementary Fig. 4a**). However, STR-2 did inhibit AChE *in vivo* (IC_{50} = 500 nM) (**Fig. 4c**). Together, these observations demonstrate that *in vivo* behavioral phenotyping in zebrafish can identify new neuroactive compounds and their mechanisms of action, including molecules that require bioactivation and would likely have been missed using *in vitro* screening assays.

In addition to clustering barcodes on the basis of phenotypic similarity, it is also possible to cluster them using small-molecule structural information. For example, we identified several structurally related coumarins that all caused a similar PMR 'magnitude stimulant' (MAG) phenotype characterized by increased PMR excitation magnitude and duration (**Fig. 4d–g** and **Supplementary Fig. 5**). To identify possible targets of the MAG compounds, we calculated their similarity against a broad panel of ligand–target sets reported as expectation (E) values[7,8]. The lowest E-values, reflecting the highest confidence predictions, were obtained for MAG-1 (**17**) against monoamine oxidase (MAO)-B, E-value 1.0×10^{-12}) and, to a lesser extent, MAO-A (E-value 9.8×10^{-9}). Other coumarins have been previously described as inhibitors of MAO-A and MAO-B[9,10]. However, no ligands with substitution patterns like those of the MAG compounds have been reported, nor have any phenotypes been described for these molecules *in vivo*. To determine whether MAG compounds inhibit MAO,

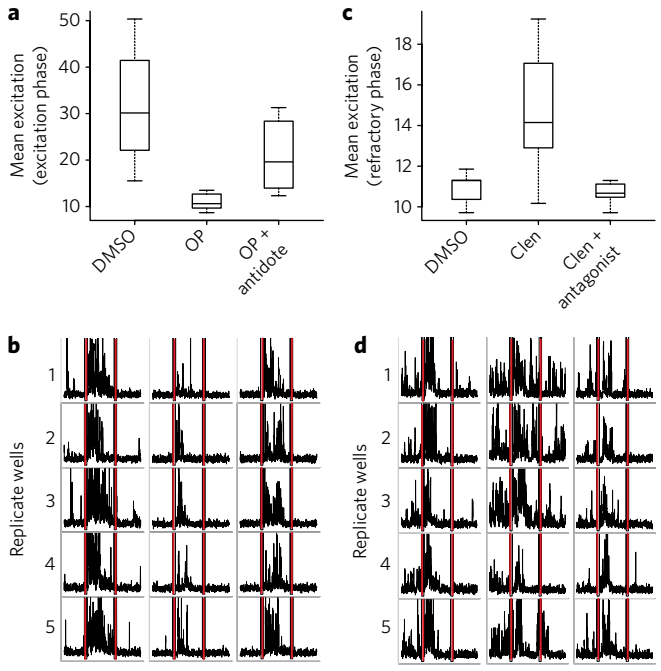

Figure 5 | Chemical suppression of behavioral phenotypes. (**a**,**b**) Box plots showing the mean excitation values (**a**) for the motion index of five replicate wells (**b**) treated with DMSO alone (vehicle control; left column), AzMet, an OP nerve poison (middle column), or AzMet plus 2-PAM and atropine (right column). (**c**,**d**) Box plots showing the mean excitation values (**c**) for the motion index of five replicate wells (**d**) treated with DMSO alone (left column), clenbuterol (Clen; middle column), or clenbuterol and the beta-receptor antagonist bopindolol (right column). For each treatment, the box in the plot represents the middle half of the distribution of the data points, stretching from the 25th percentile to the 75th percentile. The bold line across the box represents the median. The lengths of the lines above and below the box define the maximum and minimum data-point values.

we tested several of them in MAO activity assays. We found that the MAG compounds inhibited MAO *in vitro* (**Supplementary Fig. 5**) and that MAG-1 was particularly potent (IC_{50} = 1 nM), inhibiting MAO with 100 times greater potency than the known MAO inhibitor pargyline (18) (**Fig. 4h**). By contrast, high concentrations (10 μM) of the structurally related coumarin, warfarin (19), do not produce a MAG phenotype nor inhibit MAO activity. Together, these observations suggest that MAG compounds are novel MAO inhibitors.

Behavior-based chemical modifier screens

Beyond identifying molecules that affect normal behaviors, it may be possible to use high-throughput behavioral screening to identify compounds that normalize abnormal phenotypes caused by genetic mutations or pharmacological treatments. To investigate this possibility, we analyzed the suppression of behavioral phenotypes induced by molecules acting on cholinergic and adrenergic signaling pathways. Organophosphates (OP) cause seizures, paralysis and death by disrupting cholinergic signaling[11]. We found that the OP azinphos methyl (20) (AzMet) also caused paralysis in zebrafish, as evidenced by lower PMR excitation in embryos treated with AzMet than in untreated controls (**Fig. 5a**,**b**). Notably, two OP antidotes used in humans, atropine (21) and pralidoxime (22) (2-PAM), counteracted the behavioral effects of AzMet in zebrafish, restoring PMR excitation to almost normal levels (**Fig. 5a**,**b**). Similarly, the beta-adrenergic receptor antagonist bopindolol (23) was able to counteract the behavioral effects of beta-receptor agonist clenbuterol, restoring normal PMR profiles to agonist-treated embryos (**Fig. 5c**,**d**). These examples suggest that it may be possible to establish high-throughput behavioral assays in zebrafish to identify chemical modifiers of these, and possibly other, behavioral phenotypes.

DISCUSSION

So far, most pharmacological studies of behavior have been relatively small scale, involving a few small molecules at most. Here, we describe the behavioral phenotypes induced by thousands of small molecules, all tested under the same carefully controlled conditions. This large-scale data set provides opportunities for (i) systematic neuroactive drug discovery in the context of the intact nervous system and (ii) improving our understanding of how chemicals affect the brain and behavior.

Large-scale behavioral screening provides an opportunity to discover new types of neuroactive compounds for research and therapy. For example, the STR and MAG compounds described here are novel AChE inhibitors (STR-1, STR-2) or MAO inhibitors (MAG compounds) that could have therapeutic activity for treating memory loss and depression, respectively[12,13]. For each of these novel compounds, comparison with existing neuroactive drugs was central to predicting their mechanisms of action. In the case of the STR compounds, we observed that they caused behavioral phenotypes similar to those caused by known AChE inhibitors. In the case of the MAG compounds, the SEA algorithm relied upon structural similarities between the MAG compounds and existing MAO inhibitors to predict mechanisms. Not surprisingly, mechanism prediction is easiest when phenotypic or structural similarity exists between novel and known compounds. However, not all behavior-modifying compounds will have structural or phenotypic similarity to well-characterized molecules. In these cases, other target identification strategies will be necessary.

Future screens may be devised to identify compounds that suppress pharmacologically induced behavioral defects. These screens could be performed using the PMR assay or other behavioral assays. The feasibility of such an approach is supported by our observation that the PMR assay can detect the suppression of pharmacologically induced behavioral defects ranging from organophosphate-induced immobility to stimulant-induced hyperactivity (**Fig. 5**). Beyond pharmacologically induced phenotypes, it may be possible to generate genetic models of nervous system disorders and screen for small molecule modifiers of the associated behavioral defects. Recently developed technologies for targeted gene mutation in zebrafish[14–16] are likely to aid such efforts.

Behavioral assays such as the PMR may also be useful for screening chemicals for neurotoxicology or other undesirable behavioral effects. Testing drug candidates for neurotoxicity remains a significant challenge, and new regulations requiring the testing of thousands of compounds are expected to require millions of rodents and cost billions of dollars[17]. Given these costs and the ethical implications of increased animal use, inexpensive, high-throughput means of testing for neurotoxicity are needed, especially those involving nonmammalian species. Of course, questions remain about the degree of conservation of nervous-system drug effects in zebrafish and humans. Although we found that many drugs with psychotropic effects in humans also caused reproducible behavioral effects on the PMR, many other psychotropic drugs did not produce any detectable change in the PMR screen. We do not yet know the degree to which these 'false negatives' are due to screening dose, failure of absorption or imperfect conservation between zebrafish and humans. Clearly, answering these questions will be an important step toward translating behavioral pharmacology findings from zebrafish to humans.

In addition to its potential applications for drug discovery, large-scale behavior-based chemical phenotyping provides a new perspective on the relationship between small molecules and behaviors. In the experiments described here, the principal behavior under study had not previously been characterized. Despite this, the systematic approach we used has begun to provide some hints about how the

PMR is regulated. The fact that adrenergic, dopaminergic, serotonergic and other drug classes modify the PMR in distinct ways suggests that these neurotransmitter pathways all contribute to PMR regulation. In addition, the fact that specific molecules modulate individual features of the PMR (such as the response latency, the excitation magnitude, excitation duration and so forth) suggests that this poorly understood behavior comprises specific functional components under distinct mechanisms of control. This information provides testable hypotheses about the functional architecture of the behavior.

In summary, we have sought to combine the *in vivo* relevance of traditional, behavior-based phenotyping with the scale and automation of modern drug discovery. Compared to *in vitro* and cell-based assays, systematic phenotyping in living vertebrates provides a more holistic understanding of neuropharmacology, including those effects that are modulated by compound metabolism or caused by complex interactions with multiple biological pathways. Thus, behavioral barcoding in zebrafish could accelerate the pace of neuroactive drug discovery and improve our understanding of how chemicals affect the brain and behavior.

METHODS

Aquaculture. We collected a large number of fertilized eggs (up to 5,000 embryos per day) from group matings of Ekkwill or TuAB zebrafish. Embryos were raised in HEPES (10 mM)-buffered E3 medium in a dark incubator at 28 °C until 30 h after fertilization. Groups of 8–10 embryos (28 h after fertilization) were distributed into the wells of flat-bottomed, black 96-well plates filled with E3 medium (360 µl). Embryos were then incubated in a dark incubator at 25 °C for chemical treatment and subsequent experiments.

Chemical libraries. We screened the following six libraries: (i) the DiverSet library (10,000 compounds) from Chembridge; (ii) the Spectrum library (2,000 compounds) from Microsource Discovery Systems; (iii) the Prestwick library (1,120 compounds) from Prestwick Chemical; and the (iv) Neurotransmitter (700 compounds; cat. no. 2810), (v) Ion Channel (72 compounds; cat. no. 2805) and (vi) Orphan Ligand (84 compounds; cat. no. 2825) libraries from Biomol International.

Automated PMR assay and measurement. In a typical assay, 1,000 frames of digital video were recorded at 33 frames s^{-1} using a Hamamatsu ORCA-ER camera mounted on a Nikon TE200 microscope with a 1× objective. Instrument control and data measurement were performed using custom scripts for Metamorph Software (Molecular Devices). Each video was saved for review. The assay, including video recording and data processing, took ~40 s per well, enabling us routinely to screen ~500 wells (using ~5,000 embryos) per microscope-day.

To analyze digital video recordings, custom software scripts were used to automatically draw six evenly spaced line segments across each well such that each embryo is likely to be crossed by one of the lines. The software then tracks the average intensity of the pixels for each segment over time. As the embryos move, the light intensity at some of the pixels changes. A motion index is formed by taking the absolute value of the difference in average pixel intensity for adjacent time points and then summing over the six segments. This motion index correlates with the overall amount of motion in the well, both in terms of contraction frequency and number of embryos in motion.

The embryonic touch response assay. After the PMR assay, we manually touched each individual embryo in every well with a fine plastic probe and visually observed motor responses using a dissecting microscope. ETR phenotypes were categorized as normal, toxic, sedative or other. A normal ETR is characterized by brief motor activity in response to the stimulus. Toxicity was visually evaluated for developmental retardation, morphological abnormalities (brain, eye, ear, nose, somite, notochord, trunk, tail, fin), cardiovascular defects (heart morphology, heart rate, circulation), touch response and overall appearance. Wells in which embryos did not respond to the touch stimulus but appeared healthy, with strong heart beats and circulation, were annotated as 'sedative' to distinguish them from toxic compounds that may also have suppressed the normal touch response. Chemicals were annotated as 'other' if they induced some other noteworthy behavioral phenotype that was not commonly seen, including unusually strong or prolonged motor responses to the stimulus.

Chemoinformatics. We used the similarity ensemble approach (SEA) algorithms[8,18] to predict candidate molecular targets for every hit compound, using Daylight topological fingerprints[19], as previously described[8]. A filtered version of the Wombat 2006.2 database[20] (Sunset Molecular) provided a reference set of target-annotated compounds. For the clustering by chemical similarity, pairwise Tanimoto similarities were calculated between all compounds using ECFP_4 fingerprints in Pipeline Pilot version 6.1.1.0 (Accelrys).

Additional methods. For chemical treatments, light stimuli, data processing, statistical methods and enzymatic assays, see **Supplementary Methods**.

Received 11 November 2009; accepted 17 December 2009; published online 17 January 2010

References

1. Ayd, F.J. & Blackwell, B. *Discoveries in Biological Psychiatry* (Lippincott, Philadelphia, 1970).
2. Agid, Y. *et al.* How can drug discovery for psychiatric disorders be improved? *Nat. Rev. Drug Discov.* **6**, 189–201 (2007).
3. Stockwell, B.R. Chemical genetics: ligand-based discovery of gene function. *Nat. Rev. Genet.* **1**, 116–125 (2000).
4. Lehár, J., Stockwell, B.R., Giaever, G. & Nislow, C. Combination chemical genetics. *Nat. Chem. Biol.* **4**, 674–681 (2008).
5. Catterall, W.A. Cooperative activation of action potential Na+ ionophore by neurotoxins. *Proc. Natl. Acad. Sci. USA* **72**, 1782–1786 (1975).
6. Akera, T. Membrane adenosinetriphosphatase: a digitalis receptor? *Science* **198**, 569–574 (1977).
7. Hert, J., Keiser, M., Irwin, J., Oprea, T. & Shoichet, B. Quantifying the relationships among drug classes. *J. Chem. Inf. Model.* **48**, 755–765 (2008).
8. Keiser, M.J. *et al.* Relating protein pharmacology by ligand chemistry. *Nat. Biotechnol.* **25**, 197–206 (2007).
9. Gnerre, C. *et al.* Inhibition of monoamine oxidases by functionalized coumarin derivatives: biological activities, QSARs, and 3D-QSARs. *J. Med. Chem.* **43**, 4747–4758 (2000).
10. Santana, L. *et al.* Quantitative structure-activity relationship and complex network approach to monoamine oxidase A and B inhibitors. *J. Med. Chem.* **51**, 6740–6751 (2008).
11. Bajgar, J. Organophosphates/nerve agent poisoning: mechanism of action, diagnosis, prophylaxis, and treatment. *Adv. Clin. Chem.* **38**, 151–216 (2004).
12. Davis, K.L. *et al.* Physostigmine: improvement of long-term memory processes in normal humans. *Science* **201**, 272–274 (1978).
13. Thase, M.E., Trivedi, M.H. & Rush, A.J. MAOIs in the contemporary treatment of depression. *Neuropsychopharmacology* **12**, 185–219 (1995).
14. Foley, J.E. *et al.* Rapid mutation of endogenous zebrafish genes using zinc finger nucleases made by Oligomerized Pool ENgineering (OPEN). *PLoS ONE* **4**, e4348 (2009).
15. Meng, X., Noyes, M.B., Zhu, L.J., Lawson, N.D. & Wolfe, S.A. Targeted gene inactivation in zebrafish using engineered zinc-finger nucleases. *Nat. Biotechnol.* **26**, 695–701 (2008).
16. Doyon, Y. *et al.* Heritable targeted gene disruption in zebrafish using designed zinc-finger nucleases. *Nat. Biotechnol.* **26**, 702–708 (2008).
17. Rovida, C. & Hartung, T. Re-evaluation of animal numbers and costs for *in vivo* tests to accomplish REACH legislation requirements for chemicals — a report by the Transatlantic Think Tank for Toxicology (t4). *ALTEX* **26**, 187–208 (2009).
18. Holt, A. & Palcic, M.M. A peroxidase-coupled continuous absorbance plate-reader assay for flavin monoamine oxidases, copper-containing amine oxidases and related enzymes. *Nat. Protocols* **1**, 2498 (2006).
19. James, C.A., Weininger, D. & Delany, J. *Daylight theory manual* (Daylight Chemical Information Systems, 1995).
20. Oprea, T.I. *Chemoinformatics in Drug Discovery*. (Wiley, Weinheim, Germany, 2005).

Acknowledgments

We thank E. Scolnick, M. Granato, J. Dowling, D. Milan, C. Felts, J. Rihel, A. Schier and members of our research groups for encouragement and advice. This work was supported by US National Institutes of Health training grant HL07208 (D.K.) and grants NS063733 (R.T.P.), MH085205 (R.T.P.), MH086867 (R.T.P.) and GM71896 (B.K.S. and J. Irwin), the National Sciences and Engineering Council of Canada (J.B.), the Canadian Institutes of Health Research (J.B.), the Max Kade Foundation (C.L.) and the Stanley Medical Research Institute (S.J.H.).

Author contributions

D.K. designed and performed the research, analyzed the data and wrote the manuscript. J.B., C.L., R.W. and B.S. analyzed and interpreted the data and contributed to the manuscript. C.Y.J.C., R.M., D.H. and S.K. performed experiments. A.A.W. contributed to hardware design. S.J.H. and C.A.M. contributed reagents. R.T.P designed the research, analyzed the data and wrote the manuscript. All authors contributed to data interpretation and commented on the manuscript.

Competing interests statement

The authors declare no competing financial interests.

Additional information

Supplementary information and chemical compound information is available online at http://www.nature.com/naturechemicalbiology/. Reprints and permissions information is available online at http://npg.nature.com/reprintsandpermissions/. Correspondence and requests for materials should be addressed to D.K.